applied sciences

MDPI

Article

Modelling and Predicting Self-Compacting High Early Age Strength Mortars Properties: Comparison of Response Models from Full, Fractioned and Small Central Composite Designs

Nara Cangussu [1], Ana Mafalda Matos [1], Paula Milheiro-Oliveira [2,3] and Lino Maia [1,4,*]

[1] CONSTRUCT-LABEST, Faculty of Engineering, University of Porto, 4200-465 Porto, Portugal; naracan@gmail.com (N.C.); anamatos@fe.up.pt (A.M.M.)
[2] Faculty of Engineering, University of Porto, 4200-465 Porto, Portugal; poliv@fe.up.pt
[3] Mathematical Research Center (CMUP), Faculty of Sciences, University of Porto, 4099-002 Porto, Portugal
[4] Faculty of Exact Sciences and Engineering, University of Madeira, Campus da Penteada, 9020-105 Funchal, Portugal
* Correspondence: linomaia@fe.up.pt

Abstract: The mixture design of cement-based materials can be complex due to the increasing number of constituent raw materials and multiple requirements in terms of engineering performance and economic and environmental efficiency. Designing experiments based on factorial plans has shown to be a powerful tool for predicting and optimising advanced cement-based materials, such as self-compacting high-early-strength cement-based mortars. Nevertheless, the number of factor interactions required for factor scheduling increases considerably with the number of factors. Consequently, the probability that the interactions do not significantly affect the answer also increases. As such, fractioned factorial plans may be an exciting option. For the first time, the current work compares the regression models and the predicting capacity of full, fractionated (A and B fractions) and small factorial designs to describe self-compacting high-early-strength cement-based mortars' properties, namely, the funnel time, flexure and compressive strength at 24 h for the function of the mixture parameters Vw/Vc, Sp/p, Vw/Vp, Vs/Vm and Vfs/Vs for the different factorial designs. We combine statistical methods and regression analysis. Response models were obtained from the full, fractionated, and small plans. The full and fractionated models seem appropriate for describing the properties of self-compacting high-early-strength cement-based mortars in the experimental region. Moreover, the predicting ability of the full and fractionated factorial designs is very similar; however, the small design predictions reveal some concerns. Our results confirm the potentiality of fractioned plans to reduce the number of experiments and consequently reduce the cost and time of experimentation when designing self-compacting high-early-strength cement-based mortars.

Keywords: design of experiments; high strength; response model; self-compacting mortar

check for updates

Citation: Cangussu, N.; Matos, A.M.; Milheiro-Oliveira, P.; Maia, L. Modelling and Predicting Self-Compacting High Early Age Strength Mortars Properties: Comparison of Response Models from Full, Fractioned and Small Central Composite Designs. *Appl. Sci.* **2023**, *13*, 8413. https://doi.org/10.3390/app13148413

Academic Editor: Kang Su Kim

Received: 10 June 2023
Revised: 7 July 2023
Accepted: 17 July 2023
Published: 20 July 2023

Copyright: © 2023 by the authors. Licensee MDPI, Basel, Switzerland. This article is an open access article distributed under the terms and conditions of the Creative Commons Attribution (CC BY) license (https://creativecommons.org/licenses/by/4.0/).

1. Introduction

Self-compacting concrete (SCC) is distinguished by its ability to fill spaces within formwork and consolidate only by its self-weight, eliminating the need for vibration. Therefore, the final product properties of SCC elements/structures are less dependent on a worker's technical skills. As such, it has enormous potential to improve the final quality of concrete products and extend the service life of modern concrete structures [1,2].

Professor Okamura developed SCC at the University of Tokyo in the 1980s [3] to improve the durability of reinforced concrete structures associated with deficiencies in concrete compaction execution due to the shortage of skilled workers. SCC presents several advantages in terms of design, application and durability, such as (i) resource savings (in terms of manpower, equipment, and energy); (ii) the possibility of using new constructive systems with higher complexity and flexibility (reinforcement) which have a better finishing

quality; (iii) a reduction in the noise associated with the vibration process; (iv) improved quality of life, as well as health and safety on construction sites and their surroundings; and (v) the possibility of incorporating significant quantities of supplementary cementitious materials, including industrial wastes or by-products.

Over the last few decades, the scientific community has contributed to a climate of confidence in using SCC in the construction industry. Numerous researches on the subject and the vision of some European organisations (for example, RILEM and EFNARC) have ensured the technical benefits of SCC and the quality of life, health, safety and management of environmental resources. It is expected that SCC may shortly replace conventional concrete as an innovation, improving the durability and final quality of structures and potentially lowering costs [2,4–8].

Even though SCC presents exciting advantages and has attracted the interest of industry, one of the main barriers to the more widespread use of SCC is the sensitivity of the mixture to small variations in the characteristics of the constituent materials, the mix proportions and other external factors [7].

SCC constituent materials are used in vibrated concretes (VC), but in different proportions. SCC requires high fluidity and moderate cohesion. To ensure high fluidity, a superplasticiser is of utmost importance. Viscosity modifier agents and/or supplementary cementitious materials usually reach an adequate viscosity without segregation. The supplementary cementitious materials and cement form the so-called fines and, when used in appropriate proportions, improve the rheological properties of the SCC through particle packing and other hardened-state properties. As such, the mixture design of SCC may be more complex than that of vibrated concretes due to the increasing number of constituent raw materials (cement, one or more supplementary cementitious materials, viscosity-modifying admixtures, superplasticisers, and aggregates) with distinct natures and functions. Moreover, real projects are challenging nowadays, and several performance requirements are targeted for engineering, architecture, and economic and ecological impacts.

Generally, the SCC mixture design can be divided into four phases as follows [1,6]:

- Establishing the structural, constructive and environmental conditions of the application;
- The selection and characterisation of constituent raw materials;
- The preliminary SCC mixture design;
- Checking the performance requirements.

The mixture design must be revised and tested if a requirement is not checked until the desired performance is achieved. In the literature, it is possible to find a wide range of compositions that satisfy the criteria of being able to self-compact. Therefore, no single original composition exists for a given application or performance requirements. An important and decisive factor for SCC mixture design is understanding the effect of each constituent material and its interaction on the final properties of the SCC [1].

Three main types of approaches can be distinguished for SCC mixture design. The first approach is based on laboratory experiments, using the trial-and-error method. The second is based on optimising concrete paste volume, and the third approach uses statistical analyses based on factorial plans, such as the design of experiments [6,9,10].

The factorial design approach refers to planning experiments so that good-quality data can be collected and analysed using statistical methods and empirical models can be constructed that enable valid and objective conclusions and involve a minimum number of experiments. The obtained numerical models can subsequently be mathematically manipulated for various purposes, particularly for the optimisation of mixtures. In general, after formulating the problem, the factorial design involves the following steps:

1. The selection of factors (mixture parameters), levels to be considered and ranges of variation;
2. The selection of response variables;
3. The choice of the type of factorial plan;
4. Performing the experiments;
5. Performing the statistical data analysis (adjustments of a numerical model);

6. Performing further calculations involving the fitted models (optimisation) and conclusions.

Based on the method of Okamura et al. [3], the SCC mixture design can be defined by the following mixture parameters: the water-to-cement mass ratio (w/c), water-to-fines volume ratio (Vw/Vp), sand-to-mortar volume ratio (Vs/Vm), superplasticiser-to-fines mass ratio (Sp/p), the ratio between the volume of coarse aggregate and the maximum volume of coarse aggregate that can be included in 1 m^3 in the compacted state (Vg/Vg,lim) and the ratio between the sands in mass (s1/s2), if a mixture of two grains of sand is used as fine aggregate. The air content is generally fixed at 2%. Thus, all the variables except Vg/Vg,lim [1,2,7] are employed for the study of mortars. In turn, in the concrete study, only the variables related to the solid skeleton are adopted as independent variables (Vg/Vg,lim and Vs/Vm), because the paste composition remains fixed, as the result of a previous study performed at the mortar level [1,2,7].

Research Significance and Objectives

The precast industry promoted the beginning of SCC in Europe in the 1990s and applications for ready-mix concrete for bridge structures and buildings. To reduce the demoulding time and accelerate production, high-early-strength concrete compositions are typically preferred by precast companies. If self-compacting high-early-strength concrete mixtures are applied, additional advantages can be reached, namely, reducing the time needed for the demoulding strength by reducing the amount of labour in the compaction process. The recommended demoulding compressive strength ranges from 10 to 17 MPa depending on the final application [11], after a 12 to 24 h waiting period in the mould.

High-early-strength and self-compacting concrete mixtures may be challenging because they present contradicting mixture design prerequisites and fresh properties from a materials science point of view. For example, a low water/binder ratio (w/b) is crucial to attain high early strength [12]. Conversely, it may affect the mixture's self-compacting capacity, which is especially susceptible to changes in the Vw/Vp.

This work proposed a methodology for modelling and predicting high-early-strength self-compacting concrete properties by studying key properties at the mortar level (self-compacting high-early-strength cement-based mortars) using the data from [13]. Without any special curing treatment, the goal was to develop self-compacting high-early-strength cement-based mortars with 10 s of flow time and at least 50 MPa of compressive strength at the age of 24 h and with 260 mm of minimum slump flow. The five key parameters for the self-compacting high-early-strength cement-based mortars mixture chosen by [13] were as follows: (i) the water-to-powder ratio by volume, Vw/Vp; (ii) the fine-sand-to-total-sand ratio by volume, Vfs/Vs; (iii) the water-to-cement ratio by volume, Vw/Vc; (iv) the sand-to-mortar ratio by volume, Vs/Vm; and (v) the superplasticiser-to-powder ratio by mass, Sp/p. A total of 50 mixtures were produced.

As can be perceived, the number of combinations increases considerably between the number of input parameters and factors required for factor planning. Consequently, they also intensify the probability that the interactions will not significantly impact the response. As such, there is a need to reduce the time and experimentation costs [14]. For this reason, fractioned plans may be an exciting option for full factorial plans [15]. Then, this work aims to compare the response models taken from a full, fractioned, and small central composite design to describe, predict and optimise self-compacting high-early-strength cement-based mortars' properties.

2. Factorial Plan

2.1. Design

A central composite design (CCD) was preferred by Maia [13] to find the significant properties of self-compacting high-early-strength cement-based mortars explained by response models as a function of the mixture input parameters (factors). The 2^5 CCDs consisted of 32 factorial points (Fi) augmented by 10 axial points (CCi) and 8 central runs (Ci), with a total of 50 self-compacting high-early-strength cement-based mortars.

Commercially available raw materials in Portugal were employed to produce SCHSM, and the mixture proportions were translated by five independent factors (input variables): (i) Vw/Vp—water-to-powder volume ratio; (ii) Vs/Vm—sand-to-mortar volume ratio; (iii) Vw/Vc—water-to-cement volume ratio; (iv) Sp/p—superplasticiser-to-powder-mass ratio; and (v) Vfs/Vs—fine-sand-to-total-sand volume ratio.

The effect of each factor, Vw/Vc, Sp/p, Vw/Vp, Vs/Vm and Vfs/Vs, were evaluated at five levels: $-\alpha$, -1, 0, +1 and $+\alpha$, as shown in Table 1. For a rotatable design, the value of α was equal to $nF^{1/4}$, where nF is the number of factorial combinations of the design, which was 32 in the current CCD. Thus, it corresponds to $-\alpha$ and $+\alpha$, which are equal to -2.378 and +2.378, respectively. The correspondence of coded and absolute values of input mixture parameters is presented in Table 1. In addition, 14 extra points (mixtures) in the range of the CCD were produced for model validation purposes (as explained in Section 3) and are also included in Table 1 (Vi).

Table 1. Correspondence of actual and coded values of input mixture parameters.

	Units	−2.378	−1	0	+1	+2.378
X1: Vw/Vc	-	0.682	0.805	0.895	0.984	1.108
X2: Sp/p	%	0.9101	0.0217	0.0236	0.0255	0.0281
X3: Vw/Vp	-	0.4344	0.5130	0.5700	0.6270	0.7056
X4: Vs/Vm	-	0.306	0.432	0.480	0.528	0.594
X5: Vfs/Vs	-	0.043	0.250	0.400	0.550	0.757

Four response variables were analysed: (i) D-flow—slump-flow diameter; (ii) T-funnel—the time in the V-funnel; (iii) F,24h—flexural strength at the age of 24 h (the three-point loading method was applied); and (iv) Rc,24h—compressive strength at the age of 24 h [13]. The details concerning raw materials' properties, specimen production and measurement of both fresh and handed properties (response variables) can be found in [13].

2.2. Data Set

Table 2 presents the experimental findings reported by Maia [13] concerning the response variables D-flow, T-funnel, F,24h and Rc,24h. Maia [13] considered the average of two results obtained for D-flow as shown in Table 2. The F,24h has an average of 3 test records for each single mixture, and the Rc,24h has an average of 6 test records [13].

Table 2. Coded values used for determining mixtures' contents' the corresponding experimental findings are used to adjust models and CCD points for each CCD.

CCD Point	Coded Values					Responses				CCD
	Vw/Vc	Sp/p	Vw/Vp	Vs/Vm	Vfs/Vs	D-Flow [mm]	T-Funnel [s]	F,24h [MPa]	Rc,24h [MPa]	
C1	0.00	0.00	0.00	0.00	0.00	346.50	14.98	11.77	59.89	Full, A, Small
C2	0.00	0.00	0.00	0.00	0.00	346.00	13.77	12.29	62.10	Full, A, Small
C3	0.00	0.00	0.00	0.00	0.00	339.50	14.15	11.28	59.31	Full, A, B, Small
C4	0.00	0.00	0.00	0.00	0.00	348.00	14.74	12.08	60.90	Full, A, B, Small
C5	0.00	0.00	0.00	0.00	0.00	339.50	14.53	11.96	60.00	Full, A, B, Small
C6	0.00	0.00	0.00	0.00	0.00	341.00	14.38	11.89	62.17	Full, A, B
C7	0.00	0.00	0.00	0.00	0.00	345.00	13.56	11.05	60.18	Full, B
C8	0.00	0.00	0.00	0.00	0.00	344.50	14.23	11.03	59.63	Full, B
F1	−1.00	−1.00	−1.00	−1.00	−1.00	330.00	18.89	11.60	72.54	Full, B, Small
F2	1.00	−1.00	−1.00	−1.00	−1.00	349.00	12.26	11.05	57.80	Full, A
F3	−1.00	1.00	−1.00	−1.00	−1.00	338.50	16.70	12.64	70.09	Full, A
F4	1.00	1.00	−1.00	−1.00	−1.00	354.50	11.32	10.50	56.06	Full, B
F5	−1.00	−1.00	1.00	−1.00	−1.00	375.00	9.24	11.26	67.05	Full, A

Table 2. *Cont.*

CCD Point	Coded Values					Responses				CCD
	Vw/Vc	Sp/p	Vw/Vp	Vs/Vm	Vfs/Vs	D-Flow [mm]	T-Funnel [s]	F,24h [MPa]	Rc,24h [MPa]	
F6	1.00	−1.00	1.00	−1.00	−1.00	369.50	7.08	9.43	55.72	Full, B
F7	−1.00	1.00	1.00	−1.00	−1.00	376.00	7.80	10.60	68.47	Full, B
F8	1.00	1.00	1.00	−1.00	−1.00	375.00	6.91	10.18	53.40	Full, A, Small
F9	−1.00	−1.00	−1.00	1.00	−1.00	253.00	114.06	11.68	73.13	Full, A
F10	1.00	−1.00	−1.00	1.00	−1.00	289.50	38.91	11.64	58.49	Full, B
F11	−1.00	1.00	−1.00	1.00	−1.00	260.50	74.32	10.48	71.81	Full, B
F12	1.00	1.00	−1.00	1.00	−1.00	289.50	33.03	10.91	59.30	Full, A, Small
F13	−1.00	−1.00	1.00	1.00	−1.00	295.00	25.40	11.83	67.80	Full, B
F14	1.00	−1.00	1.00	1.00	−1.00	313.50	17.53	11.41	55.93	Full, A
F15	−1.00	1.00	1.00	1.00	−1.00	303.50	26.33	11.41	68.43	Full, A, Small
F16	1.00	1.00	1.00	1.00	−1.00	320.00	14.15	10.93	56.48	Full, B
F17	−1.00	−1.00	−1.00	−1.00	1.00	300.00	28.43	11.06	66.54	Full, A
F18	1.00	−1.00	−1.00	−1.00	1.00	351.50	12.89	10.69	55.93	Full, B, Small
F19	−1.00	1.00	−1.00	−1.00	1.00	334.50	17.67	11.57	69.59	Full, B
F20	1.00	1.00	−1.00	−1.00	1.00	349.50	11.73	10.73	55.10	Full, A, Small
F21	−1.00	−1.00	1.00	−1.00	1.00	378.00	9.90	11.20	65.92	Full, B
F22	1.00	−1.00	1.00	−1.00	1.00	379.50	7.16	9.93	54.52	Full, A, Small
F23	−1.00	1.00	1.00	−1.00	1.00	385.50	8.54	10.71	64.39	Full, A, Small
F24	1.00	1.00	1.00	−1.00	1.00	382.00	6.94	10.26	53.64	Full, B
F25	−1.00	−1.00	−1.00	1.00	1.00	233.00	*	12.10	67.34	Full, B
F26	1.00	−1.00	−1.00	1.00	1.00	275.00	52.64	11.42	55.30	Full, A, Small
F27	−1.00	1.00	−1.00	1.00	1.00	265.50	67.34	12.79	68.54	Full, A, Small
F28	1.00	1.00	−1.00	1.00	1.00	285.00	33.30	10.48	56.02	Full, B
F29	−1.00	−1.00	1.00	1.00	1.00	289.50	26.20	11.98	65.12	Full, A, Small
F30	1.00	−1.00	1.00	1.00	1.00	315.00	16.51	10.98	53.39	Full, B
F31	−1.00	1.00	1.00	1.00	1.00	309.00	18.57	11.88	60.96	Full, B
F32	1.00	1.00	1.00	1.00	1.00	314.00	17.07	10.66	53.41	Full, A
CC1	−2.38	0.00	0.00	0.00	0.00	168.00	*	11.91	78.42	Full, A, B, Small
CC2	2.38	0.00	0.00	0.00	0.00	342.00	11.55	10.25	48.92	Full, A, B, Small
CC3	0.00	−2.38	0.00	0.00	0.00	330.50	17.64	11.45	62.44	Full, A, B, Small
CC4	0.00	2.38	0.00	0.00	0.00	337.00	12.71	11.22	58.89	Full, A, B, Small
CC5	0.00	0.00	−2.38	0.00	0.00	295.00	79.63	12.11	64.13	Full, A, B, Small
CC6	0.00	0.00	2.38	0.00	0.00	368.50	7.27	10.18	63.04	Full, A, B, Small
CC7	0.00	0.00	0.00	−2.38	0.00	398.00	7.49	9.43	59.77	Full, A, B, Small
CC8	0.00	0.00	0.00	2.38	0.00	169.50	*	10.32	62.62	Full, A, B, Small
CC9	0.00	0.00	0.00	0.00	−2.38	338.00	16.55	Na	62.21	Full, A, B, Small
CC10	0.00	0.00	0.00	0.00	2.38	330.50	16.14	Na	57.75	Full, A, B, Small
V1	0.63	3.05	0.21	0.52	−2	320.50	16.17	11.70	58.45	Full, A, B, Small
V2	0.63	1.5	0.21	0.52	−2	327.00	16.58	11.09	60.53	Full, A, B, Small
V3	0.63	1.5	0.21	0.52	−2.67	310.50	18.33	11.17	61.54	Full, A, B, Small
V4	−0.13	0.21	−0.66	−0.62	0.00	353.00	12.96	12.02	61.33	Full, A, B, Small
V5	1.08	−0.42	−1.13	−0.62	0.00	337.50	14.09	11.47	56.70	Full, A, B, Small
V6	−1.34	0.52	−0.14	−0.62	0.00	347.00	14.15	10.35	70.59	Full, A, B, Small
V7	−0.82	0.58	−0.39	−0.62	0.00	338.50	13.64	9.68	65.96	Full, A, B, Small
V8	0.57	−0.15	−0.92	−0.62	0.00	335.00	13.02	11.16	59.11	Full, A, B, Small
V9	−0.13	−0.42	−0.66	−0.62	0.00	350.00	14.76	13.29	63.51	Full, A, B, Small
V10	−0.13	−0.42	−0.66	−0.62	0.00	344.50	15.01	11.14	65.16	Full, A, B, Small
V11	1.08	−0.42	−1.13	−0.62	0.00	346.50	14.32	11.76	57.25	Full, A, B, Small
V12	−1.34	0.52	−0.14	−0.62	0.00	344.50	15.65	13.97	72.63	Full, A, B, Small
V13	−0.82	0.58	−0.39	−0.62	0.00	345.50	15.26	13.12	68.96	Full, A, B, Small
V14	0.57	−0.15	−0.92	−0.62	0.00	347.50	15.08	Na	59.54	Full, A, B, Small

* impossible to measure/Na—result is not available.

Figure 1a depicts the T-funnel against D-flow experimental results obtained by Maia [13]. As expected, with a decrease in flow time, an increasing trend for the slump-flow diameter

is observed. The experimental plan enveloped a wide range of deformability and viscosity, with D-flow varying from 168 to 398 mm and T-funnel varying from 6.94 to 104 s. According to Okamura et al. [1] and EFNARR recommendations, self-compacting mortars must present a target D-flow between 250 and 260 mm and T-funnel of 10 s, meaning self-compatibility was reached within CCD. All D-flow and T-funnel results are also listed in the first three columns of Table 2. The CCD points F25, CC1, and CC9 do not present T-funnel values due to blocking in the V-funnel, and testing was impossible to perform.

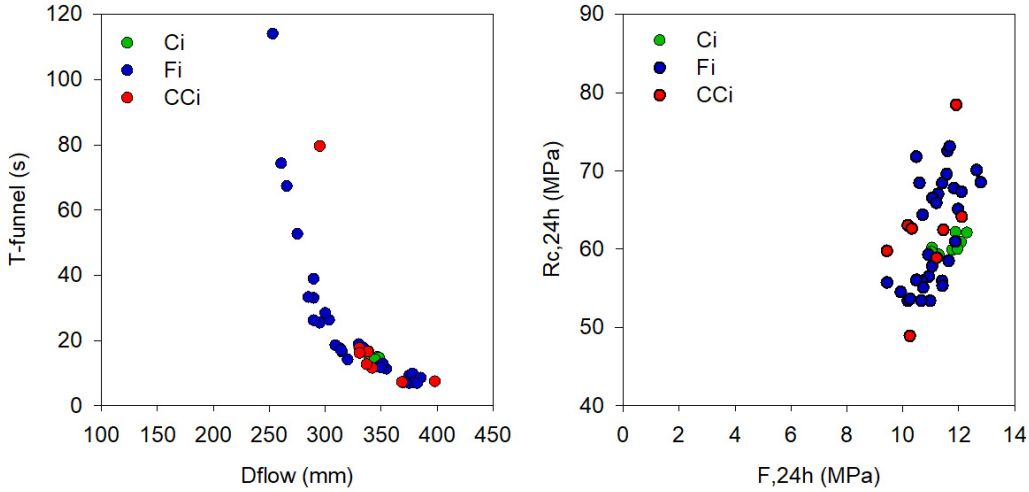

Figure 1. Results of all 50 mixtures in the CCD (**a**) D-flow and T-funnel and (**b**) F,24h and Rc,24h.

Figure 1b presents mechanical strength results. As can be seen, a scattered distribution occurred, and flexure results seem to have experienced narrow variation (9.43–12.79 MPa) while compressive strength varied between 48.92 and 78.42 MPa.

2.3. Factorial Plans Reformulation

The size of a set of experiments increases rapidly with increasing levels and factors. For example, in the factorial plan adopted by Maia [13], there were k = 5 factors corresponding to the following: 5 main effects; 10 s-order effects; 10 third-order effects; 5 fourth-order effects; and 1 fifth-order effect.

As can be perceived from Section 2.1, laboratory efforts to produce and test at least 50 mixtures (plus validation mixtures) can be hard, costly and time-consuming. Thus, in some situations, there is a need to reduce the cost of experimentation and save time, reducing the number of treatments [14]. As such, the following principle is adopted: the system is generally dominated by the main effects and the lower-order interactions. Third-order and higher-order interactions are generally neglected. Moreover, when the number of factors is high (equal to or larger than 4), it is common to perform only one point of the planning and consider the high-order interactions when estimating the error. If there is no interest in studying high-order interactions (4^{th} and 5^{th} orders), these may be disregarded, assuming that their effects are not significant and considered an error, thus originating a fractional factorial plan. The present study assumed that high-order interactions are not significant, and thus 2^{5-1} fractional factorial designs and small designs were re-formulated based on the full factorial design of Maia [13]. Small central composite designs are the designs with the minimum number of points required to estimate the terms in a second-order model. They are not rotatable and are exceptionally sensitive to outliers. Therefore, their use must be limited (see Draper and Lin (1990) [16] for details). The present work used a 3/8 fraction of the 25 factorial CCD [16].

From the full central composite design performed by Maia [13], two fractionated plans, A and B, were designed using Design expert software and a small CCD. The discrimination

of CCD points included in each plan is presented in the last column of Table 2, and the final designs are summarised in Table 3. Central points were considered as follows: C1 to C6 for fractionated plan A, C3 to C8 for fractionated plan B and C1 to C5 for small plan. Thus, 4 factorial plans were studied: Full Factorial Design (Full), Fractionated A, Fractionated B and Small, with 50, 32, 32 and 26 points, respectively.

Table 3. Central composite design plans under study: Full, Fractioned A, Fractioned B and Small.

	Full	Fractioned A	Fractioned B	Small
Factorial point	2^5 = 32	2^(5 − 1) = 16	2^(5 − 1) = 16	11
Axial points	10	10	10	10
Central points	8	6	6	5
Total points	50	32	32	26

3. Response Models

3.1. Test Results Analysis

Statistical summaries of the experimental results, presented in Table 4, were obtained in the full factorial design and for the set of the results for eight central points. A good fit for the D-flow, T-funnel and Rc,24h was predicted with the coefficient of variation on the central points (Ci) and all CCD points (all Ci, Fi and CCi). Conversely, for the coefficient of variation obtained for F,24h, when evaluating the central points (4.16%), good fits are not expected. In fact, this coefficient of variation is close to the coefficient of variation obtained for the evaluation of the 50 points of the CCD (6.93%).

Table 4. Summary statistics for full CCD and central points.

	D-Flow [mm]	T-Funnel [s]	F,24h [MPa]	Rc,24h [MPa]
		Central points		
Min	339.50	13.56	11.03	59.31
Max	348.00	14.98	12.29	62.17
Average	343.75	14.29	11.67	60.52
Std Dev	3.31	0.47	0.48	1.10
CV (%)	0.96%	3.31%	4.16%	1.81%
		Full CCD		
Min	168.00	6.91	9.43	48.92
Max	398.00	114.06	12.79	78.42
Average	323.31	22.39	11.17	61.61
Std Dev	48.97	21.63	0.77	6.24
CV (%)	15.15%	96.64%	6.93%	10.14%

Tables 5–7 report statistical summaries of the experimental results obtained for the Full, Fractionated A, Fractionated B and Small CCDs, respectively, and the results for each plan's set of central points. The coefficients of variations obtained were similar to the Full plan and predicted a suitable fit for the D-flow, t-funnel and Rc,24h. Moreover, the F,24h coefficients of variation for the Fractionated and Small plans evaluated on the central points decreased, and the coefficient of variation evaluated on the CCD increased, which indicates a good fit for the F,24h response model.

Table 5. Summary statistics for Fractionated A CCD.

	D-Flow [mm]	T-Funnel [s]	F,24h [MPa]	Rc,24h [MPa]
Fractionated A Ci points				
Min	339.50	13.77	11.28	59.31
Max	348.00	14.98	12.29	62.17
Average	343.42	14.425	11.88	60.73
Std Dev	3.84	0.43	0.34	1.20
CV (%)	1.12%	2.98%	2.88%	1.98%
Fractionated A CCD				
Min	168.00	6.91	9.43	48.92
Max	398.00	114.06	12.79	78.42
Average	321.66	23.69	11.27	61.58
Std Dev	53.11	24.15	2.88	6.18
CV (%)	16.51%	101.92%	25.59%	10.04%

Table 6. Summary statistics for Fractionated B CCD.

	D-Flow [mm]	T-Funnel [s]	F,24h [MPa]	Rc,24h [MPa]
Fractionated B Ci points				
Min	339.50	13.56	11.03	59.31
Max	348.00	14.74	12.08	62.17
Average	342.92	14.27	11.55	60.36
Std Dev	3.46	0.41	0.48	1.04
CV (%)	1.01%	2.84%	4.17%	1.72%
Fractionated B CCD				
Min	168.00	6.94	9.43	48.92
Max	398.00	79.63	12.11	78.42
Average	322.42	19.59	11.08	61.58
Std Dev	53.42	17.55	2.82	6.26
CV (%)	16.57%	89.59%	25.49%	10.17%

Table 7. Summary statistics for Small CCD.

	D-Flow [mm]	T-Funnel [s]	F,24h [Mpa]	Rc,24h [Mpa]
Small Ci points				
Min	339.50	13.77	11.28	59.31
Max	348.00	14.98	12.29	62.10
Average	343.90	14.43	11.88	60.44
Std Dev	4.08	0.48	0.38	1.09
CV (%)	1.19%	3.33%	3.22%	1.80%
Small CCD				
Min	168.00	6.91	9.43	48.92
Max	398.00	79.63	12.79	78.42
Average	322.71	21.37	11.19	61.27
Std Dev	56.15	19.11	3.15	6.20
CV (%)	17.40%	89.43%	28.16%	10.11%

3.2. Model Fitting

Statistical regression models were fitted to the data for each CCD: Full, Fractioned A, Fractioned B and Small (Table 2). Design-Expert software (Stat-Ease, Inc., Minneapolis, MN

55413-2561, USA—Design-Expert® Software, version 13.0.9.0 64-bit; Serial Number 0964-0841-3719-3394) was used to interpret the model graphically, fit an operating regression analysis and ANOVA, support the analyses of the results for each response variable by examining the summary plots of the data, and validate the model by checking the residuals for trends and outliers, autocorrelations, leverage points, and violations of the statistical assumption of the regression method. This methodology can be found in the literature, e.g., [17], in more detail. The central composite design applied allows us to estimate a full quadratic model as described in Equation (1).

$$Y = \beta_0 + \sum_{i=1}^{k} \beta_i X_i + \sum_{i=1}^{k} \beta_{ii} X_i^2 + \sum_{i<j} \sum \beta_{ij} X_i X_j + \varepsilon \quad (1)$$

where Y is the response variable; X_i corresponds to the ith design variable considered; the letter β is applied for the model parameters (β_0 is the independent term, β_i means the linear effect of X_i, β_{ii} is the quadratic effect of X_i and β_{ij} is the linear-by-linear interaction between X_i and X_j); and ε regards the fitting error. Multilinear regression analysis may assess the model parameters (β_0, β_i, β_{ij}). In the sequence of the analysis, some of the terms in Equation (1) may be considered as not significant.

The regression results when the Full CCD is used are presented in Table 8 for the response variable D-flow, as an example, due to length limitations. For more details, see reference [18]. To the best of our recollection, similarly to the previous research by [18], here, all the axial points were excluded in the multiple fit of the D-flow regression model. Thus, the quadratic model given by Eq. 1 was not able to explain the response outside the hypercube space.

Table 8. Model fit results for D-flow and T-funnel—Full plan.

Full	Fitting Model Action	Mix Nr.	Value	Reason for Action
D-flow	First action: exclude all axial mixtures	CC1	168.00	High Cook's distance as well as high leverage points.
		CC2	342.00	
		CC3	330.50	
		CC4	337.00	
		CC5	295.00	
		CC6	368.50	
		CCT	398.00	
		CC8	169.50	
		CC9	338.00	
		CC10	330.50	
T-funnel	First action: apply inverse transform	-	-	Optimisation of properties of residuals.
	Second action: exclude one factorial mixture	F15	26.33	High Cook's distance.

The regression model fit with Fractioned Plan A also presented some difficulties. A couple of runs were excluded based on the normal plot of the residuals. In the case of Fractioned Plan A for the D-flow, to reach a non-significant lack of fit, the mixtures CC1 (Std#16 Run), F17 (Std#8 Run) and CC7 (Std#22 Run) were excluded (see Figure 2). For the T-funnel, after applying an inverse transformation, one axial mixture still had to be excluded (see Figure 3). Table 9 summarises the actions undertaken for fitting the D-flow and T-funnel models for Fractioned A.

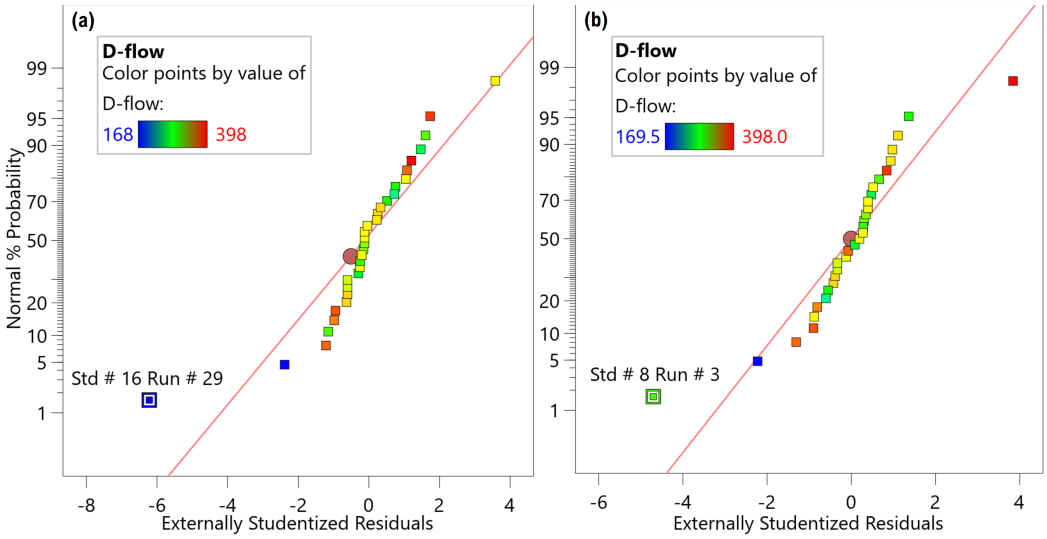

Figure 2. Normal plots of D-flow residuals for Fractioned Plan A: (**a**) all runs; (**b**) CC1 (Std#16 Run) excluded.

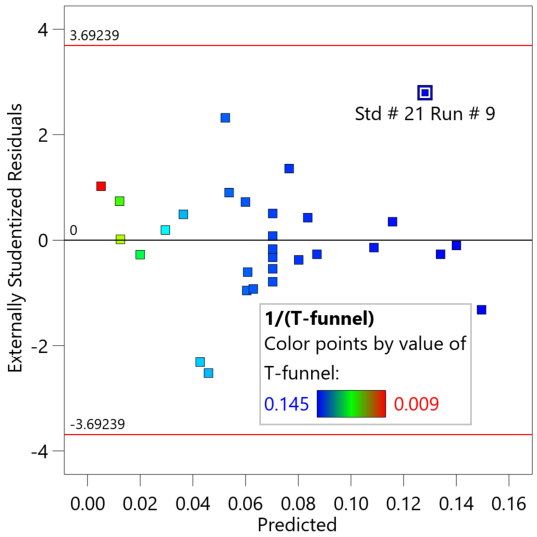

Figure 3. Fractioned Plan A: Residuals versus predicted values for T-funnel.

Table 9. Model fit results for D-flow and T-funnel—Fractioned Plan A.

Fractioned A	Fitting Model Action	Mix Nr.	Value	Reason for Action
D-flow	First action: exclude one axial mixture	CC1	168.00	Inappropriate normal plot; Residual versus predicted plot out of range.
	Second action: exclude one factorial mixture	F17	330.00	Inappropriate normal plot; Residual versus predicted plot out of range; High Cook's distance and high leverage point.
	Third action: exclude one axial mixture	CC7	398.00	Inappropriate normal plot; Residual versus predicted plot out of range; High Cook's distance and high leverage point.

Table 9. *Cont.*

Fractioned A	Fitting Model Action	Mix Nr.	Value	Reason for Action
T-funnel	First action: apply an inverse transformation	-	-	Optimisation of properties of residuals.
	Second action: exclude one axial mixture	CC6	7.27	Inappropriate normal plot; Residual versus predicted plot out of range.

In the case of Fractioned Plan A for the T-funnel, in addition to the inverse transformation, we excluded the sample CC6 (Std#21 Run—Figure 2), which was enough to prevent the model from exhibiting a significant lack of fit. Figure 3 shows graphically the T-funnel residuals versus the predicted values for Fractioned Plan A before excluding the CC6 mixture.

In case of Fractioned Plan B for the D-flow, the other half of the Full Plan, to obtain a non-significant lack of fit, two axial points were dismissed: CC1 (Std#17 Run) and CC7 (Std#23 Run) (see Figure 3). In addition, a power transform was applied to the data. Figure 4 presents the Cook's distance before and after removing these two runs.

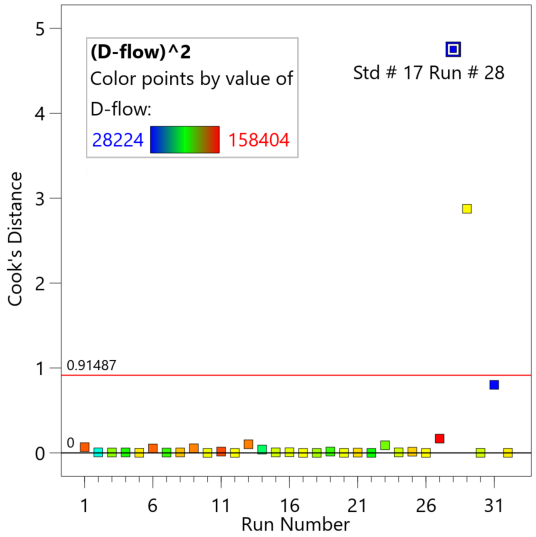

Figure 4. Cook's distance for Fractioned Plan B with all runs.

The inverse square root transformation was necessary for the T-funnel to fit the model. Table 10 describes the actions for fitting the D-flow and T-funnel models for Fractioned Plan B.

Table 10. Model fit results for D-flow and T-funnel—Fractioned Plan B.

Fractioned B	Fitting Model Action	Mix Nr.	Value	Reason for Action
D-flow	First action: apply power transformation	-	-	Optimisation of properties of residual.
	Second action: exclude one axial mixture	CC1	168.00	Normal plot show violation of normality of residuals; Residual versus predicted plot out of range; High Cook's distance.
	Third action: exclude one axial mixture	CC7	398.00	Inappropriate normal plot; Residual versus predicted plot out of range; High Cook's distance and high leverage point.
T-funnel	First action: apply inverse square root transformation	-	-	Significant lack of fit.

Excluding runs one-by-one for the fitting models, the Small plan did not respond suitably to the procedure. For this reason, all axial points for the Full plan were excluded as initially proposed. For the T-funnel Small plan, only after applying the inverse transform, as recommended for the Full plan, did the adjusted model have no significant lack of fit.

Tables 11 and 12 show the fitted models for the fresh properties (D-flow and T-funnel) and mechanical properties (F,24h and Rc,24h), using the Full, Fractioned and Small Central Composite designs previously described. The corresponding R2 and Predicted R2 values are also included. The models for the mechanical properties used all the points of each plan.

Table 11. Fitted models obtained for fresh properties, D-flow and T-funnel for Full, Fractioned and Small Central Composite designs (design variables in coded values).

	D-Flow Response Models				**T-Funnel Response Models**			
	Full	**Fractioned A**	**Fractioned B**	**Small**	**Full**	**Fractioned A**	**Fractioned B**	**Small**
Model Terms	**D-Flow [mm]**	**D-Flow [mm]**	**D-Flow^2 [mm]**	**D-Flow [mm]**	**1/(T-Funnel) [mm^{-1}]**	**1/(T-Funnel) [mm^{-1}]**	**1/(T-Funnel)^2 [mm^{-2}]**	**1/(T-Funnel) [mm^{-1}]**
Independent	343.75	338.36	1.18×108	343.9	0.0688	0.0684	1.7845	0.0683
Vw/Vc	8.92	4.5	5415.09	6.22	**0.0115**	**0.0103**	**0.6005**	**0.012**
Sp/p	4.58	NS	1681.59	5.69	0.005	0.0035	4.9076	0.0035
Vw/Vp	**19.42**	**16.28**	**11 336.31**	**18.69**	**0.0248**	**0.0223**	**2.8959**	**0.0266**
Vs/Vm	**−34.92**	**−37.37**	**−22 962.6**	**−34.7**	**−0.0302**	**−0.0325**	**1.4802**	**−0.0281**
Vfs/Vs	−1.42	NS	−403.69	NS	−0.0016	NS	−0.1572	0.0003
(Vw/Vc) × (Vw/Vp)	−5.36	NS	−3375.31	NS	NS	NS	−0.7822	NS
(Vw/Vc) × (Sp/p)	−2.89	NS	NS	NS	−0.002	NS	NS	0.0047
(Vw/Vc) × (Vs/Vm)	NS	4.51	2211.16	5.16	−0.0037	−0.0031	NS	−0.0028
(Vw/Vp) × (Vs/Vm)	3.11	NS	NS	NS	NS	NS	NS	0.003
(Vw/Vp) × (Vfs/Vs)	2.98	NS	1966.69	NS	−0.0061	−0.007	NS	−0.0111
(Sp/p) × (Vfs/Vs)	1.89	NS	NS	NS	NS	NS	NS	NS
(Sp/p) × (Vfs/Vs)	NS	NS	NS	NS	NS	NS	NS	0.0055
(Sp/p) × (Vw/Vp)	NS	NS	NS	NS	NS	NS	NS	NS
(Vs/Vm) × (Vfs/Vs)	NS	NS	−1415.59	NS	NS	NS	0.5101	NS
(Vw/Vc)2	**−20.67**	NS	−2257.79	**−19.79**	−0.0017	NS	−0.4979	−0.002
(Sp/p)2	NS	NS	1038.64	NS	NS	NS	NS	NS
(Vw/Vp)2	NS	NS	−1037.04	NS	0.0011	NS	−1.1401	0.0011
(Vs/Vm)2	NS	**−13.86**	**−5924.12**	NS	NS	−0.0019	−3.0757	NS
(Vfs/Vs)2	NS	NS	−978.97	NS	−0.0014	−0.0012	−0.1183	−0.0013
Error term (ε)								
R2	0.9858	0.9830	0.9954	0.9885	0.9922	0.9944	0.9947	0.9975
Adj-R2	0.9802	0.9793	0.9910	0.9808	0.9897	0.9916	0.9912	0.9942
Predicted R2	0.9683	0.9720	0.9753	0.9506	0.9827	0.9847	0.9709	0.9794

NS: Non-significant term. The values in bold are the three most significant parameters and the underlined ones are the most significant terms.

Table 12. Fitted models for mechanical properties F,24h and Rc,24h for Full, Fractioned and Small Central Composite designs (design variables in coded values).

	F,24h Response Models				**Rc,24h Response Models**			
	Full	**Fractioned A**	**Fractioned B**	**Small**	**Full**	**Fractioned A**	**Fractioned B**	**Small**
Model Terms	**F,24h [MPa]**	**F,24h [MPa]**	**F,24h [MPa]**	**F,24h [MPa]**	**Rc,24h [MPa]**	**Rc,24h [MPa]**	**Rc,24h [MPa]**	**Rc,24h [MPa]**
Independent	11.43	11.91	11.32	11.24	60.65	60.69	60.61	60.66
Vw/Vc	**−0.4053**	**−0.4101**	**−0.3776**	**−0.4101**	**−6.170**	**−6.180**	**−6.180**	**−6.100**
Sp/p	NS	−0.0106	NS	NS	NS	NS	NS	−0.589

Table 12. *Cont.*

	F,24h Response Models				Rc,24h Response Models			
	Full	**Fractioned A**	**Fractioned B**	**Small**	**Full**	**Fractioned A**	**Fractioned B**	**Small**
Model Terms	**F,24h [MPa]**	**F,24h [MPa]**	**F,24h [MPa]**	**F,24h [MPa]**	**Rc,24h [MPa]**	**Rc,24h [MPa]**	**Rc,24h [MPa]**	**Rc,24h [MPa]**
Vw/Vp	**−0.261**	**−0.342**	−0.2399	**−0.348**	**−1.190**	**−0.958**	**−1.020**	−0.7771
Vs/Vm	0.2608	0.2502	**0.241**	**0.309**	0.2655	0.6255	NS	0.3624
Vfs/Vs	NS	−0.0781	NS	NS	**−1.330**	**−1.200**	**−1.290**	**−1.020**
(Vw/Vc) × (Sp/p)	NS	−0.181	NS	NS	NS	NS	NS	NS
(Vw/Vp) × (Vs/Vm)	0.1826	NS	NS	NS	NS	NS	NS	NS
(Sp/p) × (Vw/Vp)	NS	−0.2173	NS	NS	NS	NS	NS	NS
(Sp/p) × (Vs/Vm)	NS	NS	NS	NS	NS	NS	NS	**1.130**
(Vs/Vm) × (Vfs/Vs)	NS	0.2585	NS	NS	−0.4934	NS	NS	NS
(Vw/Vc)2	NS	−0.1374	NS	NS	0.5639	0.5323	0.5763	0.5661
(Sp/p)2	NS	−0.0926	NS	NS	NS	NS	NS	NS
(Vw/Vp)2		−0.1265	NS	NS	0.5486	0.5169	0.5609	0.5508
(Vs/Vm)2	**−0.2834**	**−0.3501**	**−0.2659**	NS	NS	NS	NS	NS
Error term (ε)								
R2	0.6619	0.9257	0.6395	0.5230	0.9588	0.9664	0.9465	0.9800
Adj-R2	0.6216	0.8732	0.5819	0.4514	0.9519	0.9583	0.9362	0.9706
Predicted R2	0.5671	0.7782	0.5031	0.2311	0.9326	0.9203	0.8896	0.9180

NS: Non-significant term. The values typed bold are the three most significant parameters and the underlined ones are the most significant terms.

A high correlation between the response and the factors was found in the data presented in Table 12. The D-flow and T-funnel models demonstrated a strong influence of the factor Vs/Vm and Vw/Vc. As expected, the F,24h and Rc,24h models confirmed the strong influence of the factor Vw/Vc (the volume of water to the volume of cement) on the strength of the cement-based mixtures. The models also showed the inversely proportional influence of other factors containing sand, powder and water.

3.3. Model Validation

Fourteen extra mixes were proposed in Maia [13] to further validate the response models' prediction capacity. The mixture proportions of the validation mixtures are presented in the last lines of Table 2 (Vi). Vi mixtures were prepared and tested in the laboratory following the same procedures [13]. The difference between the predicted and measured results for the Fraction A, Fraction B, Full and Small plans are depicted as a box plot in Figure 5 (as percentages). Table 13 summarises the comparison between the obtained models.

From Figure 5, it can be said that the obtained models from the Fractionated A and B CCDs have a good predictive capacity based on the discrepancies between the laboratory results and the values predicted by the models. Furthermore, T-funnel had the largest range of results for almost all plans, except for Fraction A, which had the largest range of results for F,24h. The T-funnel Small plan obtained the largest differences between the predicted and measured values (over 20%). The best results, in terms of having small amplitudes and minor differences, were found for Rc,24h, followed by D-flow.

3.4. Discussion of Fitted Models Obtained

Tables 11 and 12 present the estimates of the model coefficients in coded values and denote the relative effect of the different input parameters on each response. It is well known that higher values indicate the higher influence of the design variable in the response. We recall that for each model, the three most significant parameters are typed in bold in Tables 11 and 12, and the most significant term is also underlined. A positive coefficient means that the response (or transformed response) variable will increase if the

given mixture parameter increases and vice versa. The results in Tables 11 and 12 clearly show that Vs/Vm presented the strongest (negative) effect in the response in terms of the fresh state properties D-flow and T-funnel, followed by the Vw/Vp, representing the second strongest (positive) effect. Comparing the models of each CCD, it can be perceived that the main significant factors are the same among them. For T-funnel, the three main effects are the same.

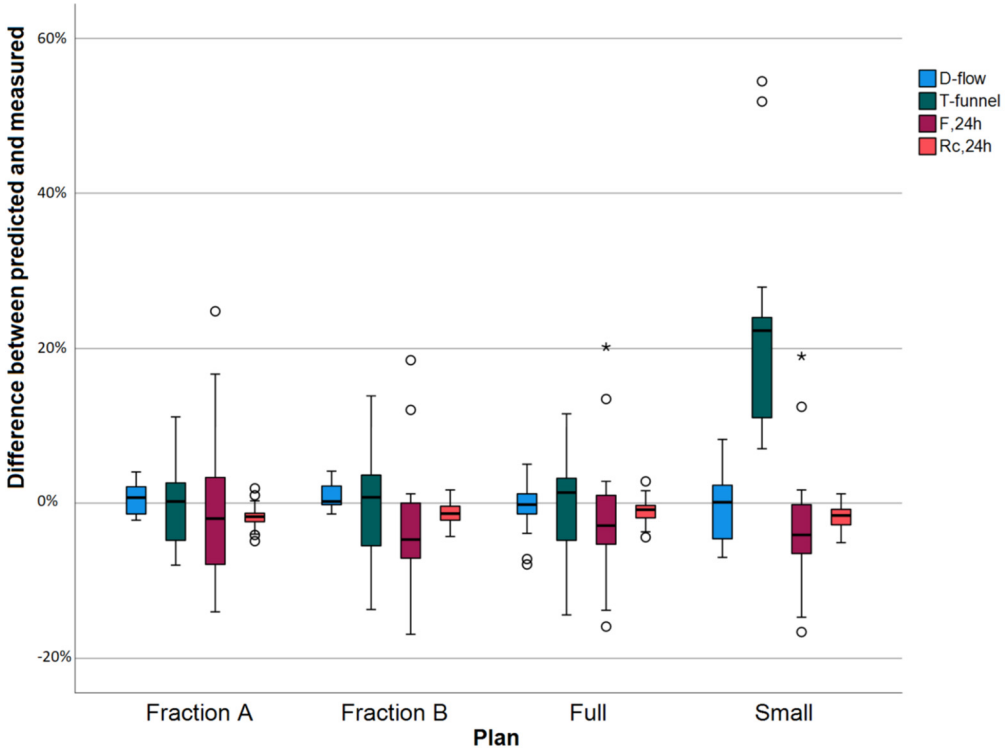

Figure 5. Box plot: Difference between predicted and measured values for Fraction A, Fraction B, Full and Small plans (° represent extreme difference values; ∗ represent outlier values).

Concerning the mechanical properties, the strongest effect is that of Vw/Vc, which is also a negative effect, as expected. By increasing the water content (Vw), the mechanical performance decreases. Vw/Vp also has a significant effect on F,24h and Rc,24h in the majority of the models. It can be noted that Vfs/Vs presents a significant negative effect on the compressive strength at 24 h.

Table 13. Summary—predicted versus measured (laboratory test) values for different designs.

	Full	Fractioned A	Fractioned B	Small
D-flow	Only two results predicted by the model showed differences between 5% and 10%. The others presented results with differences of less than 5%.	All results predicted by the model showed discrepancies of less than 5%.	All the results predicted by the model showed discrepancies of less than 5%.	Five results showed differences between 5% and 10%. The others presented results with differences of less than 5%.

Table 13. *Cont.*

	Full	Fractioned A	Fractioned B	Small
T-funnel	Almost half of the results showed discrepancies larger than 5%, with 28% of the results larger than 10%.	Almost half of the results showed discrepancies larger than 5%, with 14% of the results larger than 10%.	Half of the results showed discrepancies larger than 5%, with 21% of the results larger than 10%.	The model with the largest discrepancy between the results—in value and quantity; No result showed a difference of less than 5%. A total of 78% of the results showed discrepancies larger than 10%; The model with a larger range of results.
F,24h	A total of 35% of the results showed discrepancies larger than 10%. The others were less than 5%.	Almost half of the results showed discrepancies larger than 5%, with 35% of the results larger than 10%.	Over half of the results showed discrepancies larger than 5%, with 35% of the results larger than 10%.	Over half of the results showed discrepancies larger than 5%, with 35% of the results larger than 10%.
Rc,24h	All the model results showed discrepancies of less than 5%.	All the model results showed discrepancies of less than 5%.	All the model results showed discrepancies less than 5%.	All the model results showed discrepancies less than or equal to 5.1%.

Given the analyses presented in Table 13 and taking into account the actions developed to fit the statistics models, it can be seen that, among the designs studied, the fractioned plans were the ones that represented a good compromise between the cost of experimentation and usefulness of the statistical model obtained. Among the analysed variables, the compressive strength (Rc,24h) followed by the slump flow (D-flow) were the ones that obtained the most accurate predictions.

4. Conclusions

To understand how the input parameters affect the response variables when designing experiments, a systematic approach was used. The number of factors increase the number of interactions between the parameters necessary for factor planning dramatically. Thus, they also increase the possibilities that the interactions will not significantly influence the response. Because of this, here, fractional planning was proposed and compared with full planning for predicting self-compacting high-early-strength cement-based mortars' properties, aiming to reduce time and resources in the mixture design. Therefore, the main findings of the current work are as follows:

- For the experimentation results for the slump-flow diameter, T-funnel time, flexural and compressive strength at 24 h, the response models were considered suitable to describe self-compacting high-early-strength cement-based mortars' properties over the experimental region;
- For the slump-flow diameter and for the T-funnel time, the input parameter Vs/Vm exhibited the strongest (negative) effect in all factorial designs—Full, Fractioned A, Fractionated B and Small, followed by factor Vw/Vp;
- The regression models of the slump-flow diameter and T-funnel needed a transformation for the Fractionated B plan;

- The quadratic factor $(Vs/Vm)^2$ was found to have the main significant (negative) effect on F,24h for the Full and Fractionated A and B designs, while for the Small design, it was the factor Vw/Vp;
- The Vw/Vp was the second input parameter that most affected the Rc,24h with a negative effect for the Full and Fractionated A and B designs, while for the Small design, it was the interaction factor (Sp/p) × (Vs/Vm);
- Compared to the remaining factors, the changes in the Sp/p used in the present CCD were small. Sp/p presented the lowest influence on the self-compacting high-early-strength cement-based mortars' properties compared to the other mixture parameters for all the factorial designs evaluated.
- The models obtained from the Fractionated A and B plans have a good predictive capacity based on the discrepancies between the experimental and predicted results. The best estimated results were found for the Rc,24h response model, followed by D-flow.

Based on the aforementioned findings, the factorial plans seem to have potential applications for high-performance self-compacting mortar design and optimisation and can reduce the number of experiments as well as time and resources for experimentation.

Author Contributions: Conceptualisation, L.M.; methodology, N.C. and L.M.; software, N.C.; validation, A.M.M., P.M.-O. and L.M.; formal analysis, N.C.; investigation, N.C.; resources, L.M.; data curation, A.M.M. and P.M.-O.; writing—original draft preparation, N.C.; writing—review and editing, A.M.M. and P.M.-O.; visualisation, A.M.M.; supervision, P.M.-O.; project administration, L.M. All authors have read and agreed to the published version of the manuscript.

Funding: This work is funded by Base Funding—UIDB/04708/2020 of the CONSTRUCT—Instituto de I&D em Estruturas e Construções—funded by national funds through the FCT/ MCTES (PIDDAC); by national funds through FCT, Fundação para a Ciência e a Tecnologia, I.P., under the Scientific Employment Stimulus (Institutional Call, CEECINST/00049/2018); and national funds through FCT, Fundação para a Ciência e a Tecnologia, I.P., under individual Scientific Employment Stimulus 2021.01765.CEECIND. The author Paula Milheiro-Oliveira was partially supported by CMUP, a member of LASI, which is financed by national funds through FCT—Fundação para a Ciência e a Tecnologia, I.P., under the project UIDB/00144/2020.

Institutional Review Board Statement: Not applicable.

Informed Consent Statement: Not applicable.

Data Availability Statement: Data are contained within the article.

Acknowledgments: The authors would like to thank the funding institutions.

Conflicts of Interest: The authors declare no conflict of interest.

References

1. Nunes, S. Performance-Based Design of Self-Compacting Concrete (Scc): A Contribution to Enchance Scc Mixtures Robustness. Ph.D. Thesis, Universidade do Porto, Porto, Portugal, 2008.
2. Nunes, S.; Costa, C. Self-compacting concrete also standing for sustainable circular concrete. In *Waste and By-Products in Cement-Based Materials*; Elsevier: Amsterdam, The Netherlands, 2021; pp. 439–480. [CrossRef]
3. Okamura, H.; Ouchi, M. Self-Compacting Concrete. *J. Adv. Concr. Technol.* **2003**, *1*, 5–15. [CrossRef]
4. Domone, P.L. Self-compacting concrete: An analysis of 11 years of case studies. *Cem. Concr. Compos.* **2006**, *28*, 197–208. [CrossRef]
5. Corinaldesi, V.; Moriconi, G. Durable fiber reinforced self-compacting concrete. *Cem. Concr. Res.* **2004**, *34*, 249–254. [CrossRef]
6. Shi, C.; Wu, Z.; Lv, K.; Wu, L. A review on mixture design methods for self-compacting concrete. *Constr. Build. Mater.* **2015**, *84*, 387–398. [CrossRef]
7. Nunes, S.; Figueiras, H.; Oliveira, P.M.; Coutinho, J.S.; Figueiras, J. A methodology to assess robustness of SCC mixtures. *Cem. Concr. Res.* **2006**, *36*, 2115–2122. [CrossRef]
8. Libre, N.A.; Khoshnazar, R.; Shekarchi, M. Repeatability, responsiveness and relative cost analysis of SCC workability test methods. *Mater. Struct./Mater. Constr.* **2012**, *45*, 1087–1100. [CrossRef]
9. Khayat, K.H.; Ghezal, A.; Hadriche, M.S. Utility of statistical models in proportioning self-consolidating concrete. *Mater. Struct.* **2000**, *33*, 338–344. [CrossRef]
10. Ashish, D.K.; Verma, S.K. An overview on mixture design of self-compacting concrete. *Struct. Concr.* **2019**, *20*, 371–395. [CrossRef]

11. Ghosh, D.; Abd-Elssamd, A.; Ma, Z.J.; Hun, D. Development of high-early-strength fiber-reinforced self-compacting concrete. *Constr. Build. Mater.* **2021**, *266*, 121051. [CrossRef]
12. Feleko, B.; Türkel, S.; Baradan, B. Effect of water/cement ratio on the fresh and hardened properties of self-compacting concrete. *Build. Environ.* **2007**, *42*, 1795–1802. [CrossRef]
13. Maia, L. Experimental dataset from a central composite design to develop mortars with self-compacting properties and high early age strength. *Data Brief* **2021**, *39*, 107563. [CrossRef] [PubMed]
14. Eindhoven, T.U. Designs with a Small Number of Runs for Factorial Experiments. Ph.D. Thesis, Technische Universiteit Eindhoven, Eindhoven, The Netherlands, 1993. [CrossRef]
15. Neto, d.B.B.; Scarminio, I.S.; Bruns, R.E. *Como Fazer Experimentos*, 4th ed.; Artmed Editora SA: Porto Alegre, Brazil, 2010.
16. Draper, N.R.; Lin, D.K.J. Small Response-Surface Designs. *Technometrics* **1990**, *32*, 187–194. [CrossRef]
17. Montgomery, D.C. *Design and Analysis of Experiments*, 9th ed.; John Wiley and Sons Inc.: Hoboken, NJ, USA, 2017; Available online: https://books.google.com.br/books?id=Py7bDgAAQBAJ&lpg=PA1&ots=X7t5m4OQ59&dq=DesignandAnalysisofExperiments&lr&hl=pt-PT&pg=PA20#v=onepage&q&f=true (accessed on 31 May 2023).
18. Cangussu, N.; Matos, A.M.; Milheiro-oliveira, P. Numerical Design and Optimisation of Self-Compacting High early-Strength Cement-Based Mortars. *Appl. Sci.* **2023**, *13*, 4142. [CrossRef]

Disclaimer/Publisher's Note: The statements, opinions and data contained in all publications are solely those of the individual author(s) and contributor(s) and not of MDPI and/or the editor(s). MDPI and/or the editor(s) disclaim responsibility for any injury to people or property resulting from any ideas, methods, instructions or products referred to in the content.